

Pulsars With Jets May Harbor Dynamically Important Accretion Disks

Eric G. Blackman ¹ and Rosalba Perna ²

1. Department of Physics & Astronomy, University of Rochester, Rochester NY 14627
 2. Department of Astrophysical Sciences, Princeton University, Princeton, NJ 08544-0001
- (ApJ Lett., in press)

ABSTRACT

For many astrophysical sources with jets, there is evidence for the contemporaneous presence of disks. In contrast, pulsars such as the Crab and Vela show jets but have not yet revealed direct evidence for accretion disks. Here we show that for such pulsars, an accretion disk radiating below detectable thresholds may simultaneously account for (1) observed deviations in the braking indices from that of the simple dipole, (2) observed pulsar timing ages, and (3) possibly even the jet morphology via a disk outflow that interacts with the pulsar wind within, collimating and/or redirecting it.

Key Words: (stars:) pulsars: general; (stars:) pulsars: individual (Crab, Vela); accretion, accretion disks; ISM: jets and outflows; X-rays: ISM; plasmas

1. Introduction

Recent X-ray observations have confirmed that collimated jets can be found emanating from pulsar engines (Weisskopf et al. 2000; Helfand et al. 2001; Gaensler et al. 2002; Slane 2002; Pavlov et al. 2003). These jets morphologically resemble those of young stellar objects (Reipurth & Bally 2001), planetary nebulae, (Balick & Frank 2002) active galactic nuclei (Ferrari 1998) and microquasars (Mirabel 2001). Jets and disks are likely associated in these systems, even if the role of the disk vs. central object is not fully understood with respect to jet production. Here we explore the possibility that there may also be disks around jetted pulsars, and that winds from these disks might collimate the pulsar wind. The motivation is that relativistic pulsar winds do not seem to self-collimate easily (e.g. Lyubarsky & Eichler 2001; Bogovalov & Khangoulian 2003; Komissarov & Lyubarsky 2003): strong outward electric forces compete with the self-collimating collimating hoop stresses. Tsinganos & Bogovalov (2002) simulated the generic efficacy of relativistic wind collimation by an ambient non-relativistic wind, but did not dynamically relate the external wind to the properties of an underlying disk.

Michel & Dessler (1981) suggested that disks formed from the stellar collapse offer a physical similarity between radio and X-ray pulsars. Such disks can also influence pulsar braking indices

and timing ages: the former often deviate from those expected if spin-down were due only to dipole radiation, and the latter often differ from inferred actual ages. Various intrinsic mechanisms for these deviations have been proposed (Macy 1974; Manchester & Taylor 1977; Chanmugam & Sang 1989; Beskin et al. (1993); Chubarian et al. 2000; Wu et al. 2003), including an external torque provided by a fallback accretion disk (e.g. Menou et al. 2001a; Marsden et al. 2001; Alpar et al. 2001; Qiao et al. 2003; Shi & Xu 2003). This would imply a weaker pulsar magnetic field than that inferred from the measured period P and its derivative \dot{P} . This has been confirmed for one neutron star where the magnetic field was measured from cyclotron lines (Bignami et al. 2003).

Here we calculate the effect of a wind-emitting accretion disk on the pulsar spin evolution by coupling the latter to evolution equations for accretion and radius dependent mass loss. We constrain the pulsar magnetic field strength and the initial outer accretion rate (or disk mass) for which the solutions match the observed periods, timing ages, and braking indices of Crab and Vela. The resulting solutions produce sufficient disk-wind momenta to potentially collimate and help illuminate the pulsar winds. We describe our wind and accretion parameterization in section 2. In Sec. 3 we show that the launch mechanism determines the radial dependence of the mass outflow rate. In Sec. 4 we calculate the spin evolution of the pulsar and find best fit solutions for Crab and Vela. We compare the pulsar and disk-wind momenta in Sec. 5, and conclude in Sec. 6.

2. The accretion and disk-wind

Given the accretion rate at the outer disk radius \dot{M}_{out} , the time-dependent mass loss from a disk-wind launched between radii R_{out} and $R < R_{\text{out}}$ from the pulsar can be parameterized as

$$\dot{M}_{\text{dw}}(R, t) = \dot{M}_{\text{out}}(t) \left[1 - \left(\frac{R}{R_{\text{out}}(t)} \right)^p \right]. \quad (1)$$

(Values of $\dot{M}_{\text{out}}(t = t_0)$ and the parameter $0 < p < 1$ will be discussed below.) The accretion rate at the inner edge of the disk where the torque is exerted, is given by $\dot{M}_{\text{in}}(t) = \dot{M}_{\text{out}}(t) - \dot{M}_{\text{dw}}(R_{\text{in}}, t)$. The disk is allowed to penetrate the magnetosphere up to the magnetospheric radius¹ $R_{\text{in}} \simeq 2.55 \times 10^8 \dot{M}_{\text{in},16}^{-2/7} M_{\text{NS},1}^{-1/7} B_{12}^{4/7} \text{ cm}$ ($B_{12} 10^{12} \text{ G}$ is the pulsar's magnetic field and $M_{\text{NS},1} M_{\odot}$ its mass) where the torque exerted by the magnetic field on the disk is of order the viscous torque.

To constrain $\dot{M}_{\text{out}}(t)$, we appeal to previous work. Chevalier (1989) studied fallback accretion, but without angular momentum. Here we adopt the Menou et al. (2001a; see also Chatterjee et al. 2000) analogy between fallback accretion and accretion of the torus of gas formed by a disrupted star (Cannizzo et al. 1990). Cannizzo et al. (1990) showed that there is a transient spreading phase of duration t_0 during which the accretion is nearly constant, $\dot{M}_{\text{out}}(t) \sim \dot{M}_{\text{out}}(t_0)$ but after

¹The surface where the pulsar field develops a significant toroidal component (facilitating a Poynting flux outflow) likely has an hourglass shape, being pinched at the disk midplane. Field lines extending from the pulsar to large distances would develop toroidal fields closer to the light cylinder, due to the rapid density drop away from the disk.

which the accretion rate declines as a power-law with time, $\dot{M}_{\text{out}}(t) = \dot{M}_{\text{out}}(t_0)[t/t_0]^{-\delta}$, and the initial accretion rate depends linearly on the product of the viscosity parameter α_{ss} (Shakura & Sunyaev 1973) and the initial mass of the disk. They also found that $\delta = 19/16$ provides a good fit to the late time evolution and that the outer edge of the disk then evolves as $R_{\text{out}} \propto (t/t_0)^{3/8}$. The initial R_{out} is determined by the angular momentum of the presupernova star and the amount of ejected material. Menou et al. (2001b) estimate $R_{\text{out}}(t_0) \approx 10^6 - 10^8$ cm for the typical angular momentum in the presupernova star found in numerical simulations (Heger, Langer & Woosley 2000). The time t_0 satisfies $t_0 \simeq 300 \left(\frac{\alpha_{ss}}{0.1}\right)^{-1} \left(\frac{H_{\text{out}}/R_{\text{out}}}{0.1}\right)^{-2} \left(\frac{R_{\text{out}}(t_0)}{10^7 \text{ cm}}\right)^{3/2} \left(\frac{M_{\text{NS}}}{M_{\odot}}\right)^{-1/2}$ sec, the viscous infall time at $R_{\text{out}}(t_0)$, where H_{out} is the outer disk height.

From (1), we can also write the total mechanical disk-wind luminosity as

$$L_{\text{dw}}(t) = \frac{1}{2} \int_{R_{\text{in}}}^{R_{\text{out}}} \frac{d}{dR} (\dot{M}_{\text{dw}}(R, t) V_{\text{dw}}^2) dR \simeq \frac{GM_{\text{NS}} \left(\frac{V_{\text{dw}}(R_{\text{in}})}{V_{\text{esc}}}\right)^2 \dot{M}_{\text{out}}(t) \left[1 - \left(\frac{R_{\text{in}}}{R_{\text{out}}}\right)^p\right]}{R_{\text{in}}(t)}. \quad (2)$$

where V_{esc} is the escape speed at the inner radius, and the last step holds when the total mass inside radius R satisfies $M_{\text{tot}}(R, t) \leq M_{\text{NS}}R/R_{\text{in}}$. Note that the initial total disk mass is $\sim \dot{M}_{\text{out}}(t_0)t_0$, so our equations could be scaled in terms of this quantity.

3. How p can be constrained from disk-wind theory

For magnetically mediated outflows (e.g. Spruit 1996), the mechanical wind luminosity is powered by Poynting flux from large scale fields. The associated magnetic luminosity is

$$L_{\text{dw}} = \frac{c}{4\pi} \int_{R_{\text{in}}}^{R_{\text{out}}} (\overline{\mathbf{E}} \times \overline{\mathbf{B}}) 2\pi R dR = \frac{1}{2} \int_{R_{\text{in}}}^{R_{\text{out}}} V_{\phi} \overline{B}_z \overline{B}_{\phi} R dR, \quad (3)$$

where $\overline{\mathbf{E}}$ is the mean surface electric field, \overline{B}_z and \overline{B}_{ϕ} are the surface components of the mean magnetic field, and V_{ϕ} is the Keplerian speed. The surface magnetic fields in (3) can be related to the fields in the disk by using the volume integral $\int \nabla \cdot \overline{\mathbf{B}} dV = 0$ taken over a wedge in the disk and converting to a surface integral. Using this, Tan & Blackman (2003) showed that if large scale disk fields are obtained from a helical dynamo, driven by disk turbulence and shear, the surface magnetic stress takes the form $\overline{B}_z \overline{B}_{\phi} \sim 4\pi \rho c_s^2 \alpha_{ss}^{3/2} (H/R)$, where c_s is the mid-plane sound speed, H is the disk height and ρ is the mid-plane density. (The proportionality to $4\pi \rho c_s^2$ would arise for any helical or non-helical dynamo, but the $\alpha_{ss}^{3/2}(H/R)$ factor would be replaced by α_{ss} if we used the averaged turbulent magnetic stress rather than the magnetic stress associated with the large scale fields.) Combining this magnetic stress with $\rho = \frac{\dot{M}_{\text{in}}}{4\pi R H V_r}$, the equation for $\dot{M}_{\text{in}}(t)$, the disk scalings (e.g. Frank et al. 2002) $V_r \simeq \alpha_{ss} c_s \frac{H}{R} \simeq \alpha_{ss} V_{\phi} \frac{H^2}{R^2}$, and plugging the result into (3) gives

$$\frac{1}{2} \int_{R_{\text{in}}}^{R_{\text{out}}} \frac{\alpha_{ss}^{1/2} \dot{M}_{\text{in}} V_{\phi}^2}{R} dR = \frac{\alpha_{ss}^{1/2} GM_{\text{NS}} \dot{M}_{\text{out}}}{2R_i (R_{\text{out}}/R_{\text{in}})^p} \int_1^{\lambda_o} \lambda^{p-2} d\lambda. \quad (4)$$

The last equation follows from the expression for $M_{\text{in}}(t)$, $V_\phi = (GM_{\text{NS}}/R)^{1/2}$, and defining $\lambda \equiv R/R_{\text{in}}$ and $\lambda_o \equiv R_{\text{out}}/R_{\text{in}}$. We can set (4) equal to (2), to obtain

$$(1-p)(\lambda_o^p - 1) = (1-p) \left(\frac{V_{\text{esc}}}{V_{\text{dw}}} \right)^2 \frac{\alpha_{ss}^{1/2}}{2} \int_1^{\lambda_o} \lambda^{p-2} d\lambda = \left(\frac{V_{\text{esc}}}{V_{\text{dw}}} \right)^2 \frac{\alpha_{ss}^{1/2}}{2} (1 - \lambda_0^{p-1}). \quad (5)$$

Eqn. (5) shows that p is not independent of $V_{\text{dw}}/V_{\text{esc}}$ and α_{ss} once a launch mechanism is chosen. The above formalism involves the relation that the mechanical disk-wind luminosity at a given radius is a constant fraction of the accretion luminosity, so Ref (4) implies that both L_{dw} and the accretion luminosity increase with decreasing p if all other quantities were fixed. This formalism breaks down when the value of p is so low that $V_{\text{dw}} \rightarrow c$.

4. Pulsar spin-down

The pulsar dipole luminosity for a neutron star of angular speed Ω and radius R_{NS} is given by

$$L_{\text{pul}}(t) \simeq \frac{B_*^2 \Omega^4(t) R_{\text{NS}}^6}{6c^3}, \quad (6)$$

where $B_* \equiv B \sin \theta$, and θ is the angle between the magnetic and spin axes. We have not considered the time evolution of $\sin \theta$ here. This was studied by Beskin et al. (1993) and could be included in future generalizations. The rotational energy evolution is determined by this dipole radiation and a model dependent accretion torque so that

$$\dot{E} = I\Omega\dot{\Omega} = -\beta\Omega^4 + 2\dot{M}_{\text{in}}R_m^2\Omega\Omega_{\text{K}}(R_m) \left[1 - \frac{\Omega}{\Omega_{\text{K}}(R_m)} \right]^\gamma, \quad (7)$$

where I is the moment of inertia of the star, $\beta \equiv B^2 \sin^2 \theta R_{\text{NS}}^6/6c^3$, and we use a $\gamma = 1$ model. We also define the braking index and timing age as $n(t) \equiv \frac{\Omega\ddot{\Omega}}{\dot{\Omega}^2}$ and $T(t) \equiv \frac{\Omega}{2\dot{\Omega}}$ respectively.

We determine the spin evolution of the star by numerically solving Eq. (7) combined with the equations in section 2. To do so, we also need the pulsar's magnetic field, the initial spin period, and the initial accretion rate in the disk. If the star were spinning down only by dipole radiation, then its magnetic field would be directly determined from measuring P and \dot{P} . But when a disk torque contributes to the spin-down, we only know that the magnetic field strength must be smaller than the value obtained for a pure dipole. For young pulsars, we expect $10^{11} \lesssim B \lesssim 10^{13}$ G. The initial spin period P_i is also uncertain, but typically, $1 \lesssim P_i \lesssim 20$ msec. The initial accretion rate is likewise unknown. To constrain these parameters in our model, we use observational values of the period, timing age and braking index for the specific pulsar under consideration. We then solve the coupled system of equations using a grid of values for P_i , $\dot{M}_{\text{out}}(t_0)$ and B_* to obtain a best fit parameter range that reproduces the observed values of P , T and n to within a few percent.

We specifically consider the Crab and Vela pulsars. In 1972, the Crab's true age was 918 yr, and its measured timing age was $T = 1243$ yr, while the braking index was $n = 2.51$ with period

$P = 33.1$ ms. Vela has a braking index of $n = 1.4 \pm 0.2$ (Lyne et al. 1996), a period $P = 89$ ms, and a timing age $T = 11.3$ kyr, for a pulsar age (determined from the associated supernova remnant; Aschenbach, Egger & Trumper 1995) in the range 18-30 kyr. Here we use ~ 25 kyr.

Fig. 1a shows two solutions ($p = 0.5$ and $p = 0.01$) for the Crab, which reproduce the measured values of P , T and n . The $p = 0.5$ solution was obtained with $B_* = 1.5 \times 10^{12}$ G, $P_i = 17.7$ msec, and $\dot{M}_{\text{out}}(t_0) = 10^{29}$ g/s, while that with $p = 0.01$ has $B_* = 1.7 \times 10^{12}$ G, $P_i = 17.4$ msec, and $\dot{M}_{\text{out}}(t_0) = 9.1 \times 10^{27}$ g/s. The bottom panel displays the pulsar and wind luminosities [Eq.(6) and Eq.(2)] during the pulsar lifetime. Fig. 1b shows, for the same values of p , the solutions for Vela which reproduce its observations within the measurement uncertainties. The solution with $p = 0.5$ was obtained with $B_* = 7.7 \times 10^{11}$ G, $P_i = 7.9$ msec, and $\dot{M}_{\text{out}}(t_0) = 3 \times 10^{30}$ g/s, while that with $p = 0.01$ has $B_* = 7.6 \times 10^{11}$ G, $P_i = 7.9$ msec, and $\dot{M}_{\text{out}}(t_0) = 4.7 \times 10^{29}$ g/s². Also displayed are the pulsar and wind luminosities, and the observed lower limit on the jet luminosity. Pavlov et al. (2003) estimated an energy injection rate $\gtrsim 8 \times 10^{33}$ g/s for the Vela jet. In all of our solutions, the corotation radius is less than the magnetospheric radius at all times, so the pulsars are always spun down by the disk. The precise value of p is not crucial to obtain a good solution for P , T and n ; what matters for the spin-down torque is the value of \dot{M}_{in} , and a different p can be compensated with a different \dot{M}_{out} to yield a similar \dot{M}_{in} (and hence a similar evolutionary track). This is why the two lines in the top three panels of Fig.1 overlap. Note that the higher p curves for L_{dw} are *above* the lower p curves because \dot{M}_{out} is larger for the larger p cases, and this counteracts the dependence of L_{dw} on p discussed below Eq. (5).

The particular solutions in Fig. 1 are not unique; multiple combinations of the parameters B , P_i and $\dot{M}(t_0)$ can reproduce the values of P , T and n within the observational uncertainties. However, we have shown solutions that also produce a disk-wind powerful enough to influence the jets observed in these sources, as discussed in more detail in the next section. For the solutions of Fig. 1, $R_{\text{in}} \sim 9 \times 10^7$ cm and $R_{\text{out}} \sim 6 \times 10^9$ cm for Crab and $R_{\text{in}} \sim 10^8$ cm and $R_{\text{out}} \sim 10^{10}$ cm for Vela. For the Crab, the predicted optical emission from an even a face-on thin disk³ would be below the optical detection (Sollerman 2003). For Vela, the observed optical flux limits require either (i) a disk almost edge-on to the line of sight (ii) disruption of the outer parts of the disk (maybe through interaction with the supernova remnant) or (iii) a geometrically thick and optically thin disk, like an advection dominated accretion flow (ADAF) (e.g. Esin et al. 1997).

²Multiplying t_0 with $\dot{M}_{\text{out}}(t_0)$ from our fits gives initial disk masses $\sim 0.01 - 0.5 M_{\odot}$. The values of $\dot{M}_{\text{out}}(t_0)$ in our formal solutions, like those in accretion models of gamma-ray bursts, are highly super-Eddington. Such disks would be dense, hot, and thick from radiation trapping (Di Matteo et al. 2002). Here the Cannizzo et al. (1990) similarity solutions may be inapplicable, but this does not strongly affect the present day pulsar parameter solutions.

³The present day disk is assumed to be optically thick, geometrically thin, and both viscous dissipation and irradiation by the pulsar are included (Perna et al. 2000; Perna & Hernquist 2000).

5. Effect of the disk-wind on the jet

Relativistic Poynting flux pulsar winds do not easily self-collimate (e.g. Lyubarsky & Eichler 2001); as strong outward electric forces compete with the collimating magnetic hoop stress. (This problem would not arise in non-relativistic outflows, as the electric field << magnetic field.) We suggest instead that pulsar jets may be collimated by a surrounding disk wind.

A necessary condition for the disk wind to collimate the pulsar wind is that the ram pressure associated with the disk wind exceed the magnetic pressure associated with the Poynting flux dominated pulsar wind on scales at or less than those where the collimation is observed. Since the jets appear on scales \gg than that of the disk, it is reasonable to make this comparison far outside the pulsar's light cylinder. Magnetic energy dominates the particle energy in the pulsar wind, so the energy outflow rate can be estimated as $L_{\text{pul}} \sim c(B^2/8\pi)4\pi r^2$, where r is a spherical radius. Comparing the two pressures amounts to comparing $B^2/8\pi$ to $\dot{M}_{\text{dw}}(t)V_{\text{dw}}/8\pi r^2$. But $B^2 r^2 = L_{\text{pul}}/2c$, so this amounts to comparing $\dot{M}_{\text{dw}}V_{\text{dw}} = L_{\text{dw}}/V_{\text{dw}}$ with L_{pul}/c , namely comparing the rate of change of the disk-wind momentum to that of the pulsar wind.

Fig. 2 shows precisely this comparison for Crab and Vela. The solutions indicate that a collimating influence of the disk-wind on the pulsar wind is possible for the $p = 0.5$ case for both pulsars. That $p = 0.5$ provides higher disk-wind momenta and higher $L_{\text{dw}}/L_{\text{pul}}$ than $p = 0.01$ results because the \dot{M}_{out} which best fits the spin parameters is larger for the large p cases. (For the same \dot{M}_{out} , the large p case would have a lower L_{dw} and momentum than the low p case, as discussed below Eq. (5).) Although this effect dominates, a competing effect is that $V_{\text{dw}}(R)$ increases with decreasing p : for both pulsars, Eq. (5) for $\alpha_{ss} = 0.1$ reveals that $p = 0.5$ and $p = 0.01$ correspond to $V_{\text{dw}}/V_{\text{esc}} \sim 0.2$ and $V_{\text{dw}}/V_{\text{esc}} \sim 2$ respectively. Collimation also requires that the vector sum of the pulsar wind and disk wind momenta incurs a significant vertical component. Even if the disk wind were spherical, when its ram pressure exceeds that of the pulsar wind the pulsar wind would incur some collimation. However, since the disk wind is largely non-relativistic, magnetic self-collimation of the disk wind is not as problematic as that of the pulsar wind. Self-collimation of the disk wind would favor even more collimation of the pulsar wind. A more detailed model of the interacting outflows is required to further develop these ideas. Note that Tsinganos & Bogovalov (2002) have found numerically that relativistic central outflows could in principle be collimated by non-relativistic disk winds, also motivating more detailed models. A standard limitation of such numerical calculations is the assumption of the disk field geometry as a given initial condition.

At the interface of the two winds, significant dissipation can occur, and accelerated particles can produce the observed radiation. In addition, bending of the collimated jet could result from mutual non-axisymmetry of coaxial winds, or from misaligned pulsar and disk wind symmetry axes. Pavlov et al. (2003) suggested that a hidden wind from within the supernova remnant is needed to account for Vela's bent jet.

6. Conclusions

Winds from fallback accretion disks below presently detectable limits may deposit enough momenta to collimate and bend the Crab and Vela pulsar winds and account for their observed jets. These disks can also account for the observed periods, braking indices, and timing ages of the Crab and Vela pulsars through the action of the disk torque on pulsar spin-down. Our results motivate further efforts to detect disks around jetted pulsars, and more detailed models of the nested interacting winds. Collimating a relativistic central wind by a surrounding accretion disk-wind may also be a relevant paradigm for active galactic nuclei and gamma-ray bursts.

We thank L. Hernquist, K. Menou, and the referee for useful comments.

REFERENCES

- Alpar, M. A., Ankay, A., Yazgan, E. 2001, ApJ, 557L, 61
Aschenbach, B., Egger, R., & Trumper, J. 1995, Nature, 373, 587
Balick, B. & Frank, A. 2002, ARAA, 40, 439
Bignami, G. F., Caraveo, P. A., De Luca, A., Mereghetti, S. 2003, Nature, 423, 725
Bogovalov, S. V.; Khangoulian, D. V. 2003, MNRAS, 336L, 53
Beskin V.S., Gurevich A.V., Istomin Ya. N, 1993 “Physics of the Pulsar Magnetosphere”
(Cambridge Univ. Press: Cambridge)
Cannizzo, J.K., Lee, H.M. & Goodman, J. 1990, ApJ, 351, 38
Chanmugam, G. & Sang, Y. 1989, MNRAS, 241, 295
Chatterjee, P., Hernquist, L. & Narayan, R. 2000, ApJ 534, 373
Chevalier, R. A. 1989, ApJ, 346, 847
Chubarian, E., Grigorian, H., Poghosyan, G., & Blaschke, D. 2000, A&A, 357, 968
Di Matteo, T., Perna, R., Narayan, R. 2002, ApJ, 579, 706
Esin A. A., McClintock J.E., Narayan R., 1997, ApJ, 489, 865
Ferrari, A. 1998, ARAA, 36, 539
Gaensler, B. M., Arons, J., Kaspi, V. M., Pivovaroff, M. J., Kawai, N., & Tamura, K. 2002, ApJ, 569, 878
Heger, A.; Langer, N.; Woosley, S. E. 2000, ApJ, 528, 368
Helfand, D. J., Gotthelf, E. V., & Halpern, J. P. 2001, ApJ, 556, 380
Frank, J., King, A., & Raine, D. J. 2002, *Accretion Power in Astrophysics*, (Cambridge University Press: Cambridge UK).

- Komissarov, S. S. & Lyubarsky, Y. E., preprint astro-ph/0306162
- Lyne, A.G., Pritchard, R.S., Graham-Smith, F. & Camilo, F. 1996, Nature, 381, 497
- Lyubarski, Y. & Eichler, D. 2001, ApJ, 562, 494
- Macy, W.W., 1974, ApJ, 190, 153
- Manchester R.N. & Taylor J.H., 1977, *Pulsars*, (Freeman: San Francisco).
- Marsden, D., Lingenfelter, R.E. & Rothschild, R.E. 2001a, ApJL,
- Menou, K., Perna, R. & Hernquist, L. 2001a, ApJ, 554L, 63
- Menou, K., Perna, R. & Hernquist, L. 2001b, ApJ, 559, 1032
- Michel, F. C. & Dessler, A. J. 1981, ApJ, 251, 654
- Mirabel, I. F. 2001, Astrophysics and Space Science Supplement, 276, 319
- Pavlov, G. G.; Teter, M. A.; Kargaltsev, O.; Sanwal, D. 2003, ApJ, 591, 1157
- Perna, R., Hernquist, L., & Narayan, R. 2000, ApJ, 541, 344
- Perna, R. & Hernquist, L. 2000, ApJ, 544, L57
- Reipurth, B. & Bally, J. 2001, ARAA, 39, 403
- Sollerman, J. astro-ph/0306188
- Qiao, G. J., Xue, Y. Q., Xu, R. X., Wang, H. G., Xiao, B. W., astro-ph/0306489
- Shakura, N. I. & Sunyaev, R. A. 1973, A&A, 24, 337
- Shi, Y. & Xu, R. X. 2003, ApJL in press, astro-ph/0307113
- Slane, P. 2002, ASP Conf. Ser. 271: Neutron Stars in Supernova Remnants, 165
- Spruit, H. C. 1996, in NATO ASI Proc. 477: *Evolutionary Processes in Binary Stars*, 249, eds. R.A.M.J. Wijers, M.B. Davies and C.A. Tout, (Kluwer: Dordrecht)
- Tsinganos K. & Bogovalov S., 2002, MNRAS 337, 553.
- Tan, J. C. & Blackman, E.G., 2003, submitted to ApJ, astro-ph/0307455
- Weisskopf, C., et al. 2000, ApJ, 536, L81
- Wu, F., Xu, R. X., Gil, J. 2003, A&A, 409, 641

Fig. 1: Evolution of the period, braking index, timing age, dipole luminosity and disk-wind luminosity for Crab and Vela. The points mark the observed values, though no such constraints exist for the Crab jet power. The age for Vela is taken to be that of the associated supernova remnant. Boldface lines correspond to $p = 0.5$ and thin lines to $p = 0.01$. Results are rather insensitive to the value of p .

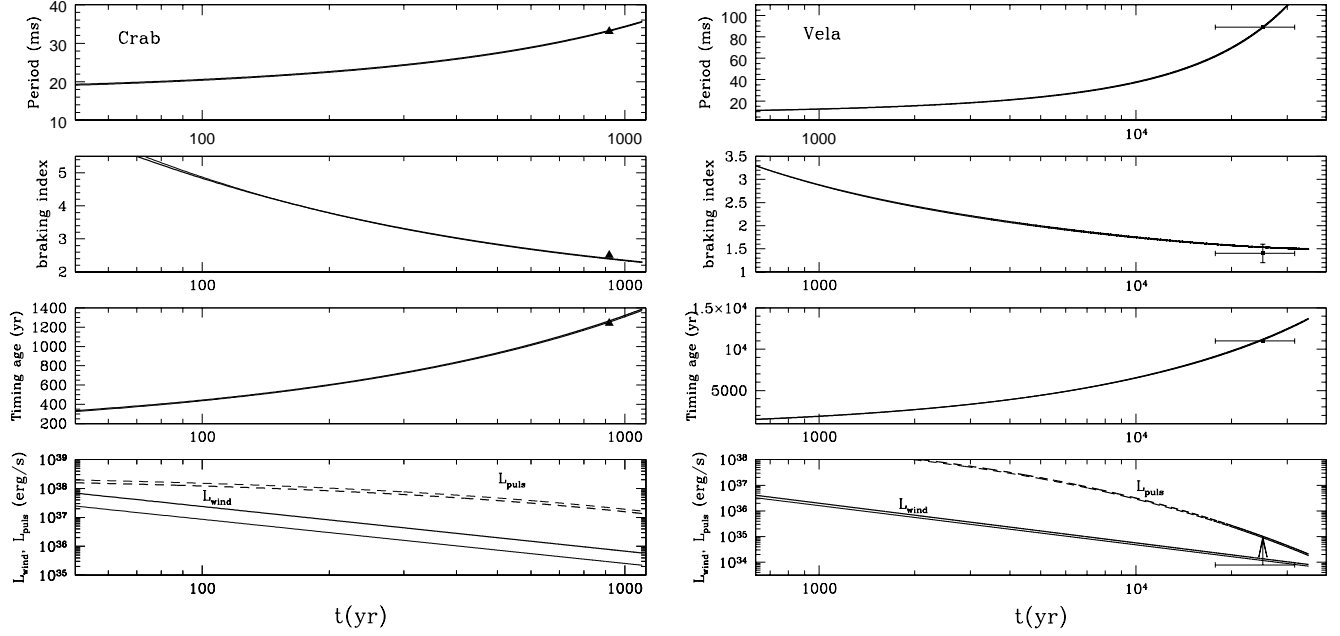


Fig. 2: Momentum per unit time ejected by the disk-wind compared to that associated with the pulsar’s Poynting flux. Boldface lines correspond to $p = 0.5$ and thin lines to $p = 0.01$.

